

# Effect of top quark spin on the unparticle couplings in $\gamma\gamma \rightarrow t\bar{t}$

İnanç Şahin\*

*Department of Physics, University of Wisconsin, Madison, WI 53706, USA and*

*Department of Physics, Faculty of Sciences,*

*Ankara University, 06100 Tandogan, Ankara, Turkey*

## Abstract

We investigate the potential of  $\gamma\gamma$  collisions to probe scalar unparticle couplings via top-antitop quark pair production. We find 95% confidence level limits on the unparticle couplings with an integrated luminosity of  $500fb^{-1}$  and  $\sqrt{s} = 1$  TeV energy. We investigate the effect of top quark spin polarization on the unparticle couplings. It is shown that spin polarization of the top quark leads to a significant improvement in the sensitivity limits.

PACS numbers: 14.80.-j, 14.65.Ha, 13.88.+e

---

\*isahin@wisc.edu; isahin@science.ankara.edu.tr

## I. INTRODUCTION

Scale invariance plays a crucial role in theoretical physics. A possible scale invariant hidden sector that may interact weakly with the Standard Model (SM) fields is being discussed intensively in the literature. Based on a scale invariant theory by Banks-Zaks (BZ) [1], Georgi proposed a new scenario [2, 3] in which SM fields and a scale invariant sector described by (BZ) fields interact via the exchange of particles with a large mass scale. At low energies this scale invariant sector manifests itself as a non-integral number  $d_U$  of particles called unparticles. Several effective interaction terms between unparticles and SM particles have been proposed and phenomenological [4], astrophysical and cosmological [5] implications of unparticles have been intensively studied in the literature.

The top quark possesses a large mass; its mass is at the electroweak symmetry-breaking scale. Because of its large mass, top quark couplings are expected to be more sensitive to new physics than other particles [6]. Probing top quark couplings in the context of new physics will be a crucial test of the SM. Top quark couplings to unparticles have been analyzed in several papers without taking into account of top quark spin polarization [7, 8]. Because of its large mass the weak decay time for the top quark is much shorter than the typical time for the strong interactions to affect its spin [9]. Therefore, the information on its polarization is not disturbed by hadronization effects but transferred to the decay products. The effect of top quark spin polarization on a possible new physics contribution from extra dimensions and several effective Lagrangians have been widely studied in the literature. Top spin analysis in the top-antitop pair production processes has been performed regarding ADD and RS models [10] and the effective Lagrangian approach [11].

In this paper, we investigate the scalar unparticle contribution in the process  $\gamma\gamma \rightarrow t\bar{t}$ . We take into account top spin polarization along the direction of various spin bases to improve the sensitivity bounds. We have shown that top spin polarization leads to a significant improvement in the sensitivity bounds.

In our calculations we consider the following effective interaction operators between SM fields and scalar unparticles [12]:

$$\frac{\lambda_S}{\Lambda_U^{d_U-1}} \bar{f} f O_U, \quad \frac{\lambda_{PS}}{\Lambda_U^{d_U-1}} \bar{f} i \gamma^5 f O_U, \quad \frac{\lambda_V}{\Lambda_U^{d_U}} \bar{f} \gamma^\mu f (\partial_\mu O_U), \quad \frac{\kappa}{\Lambda_U^{d_U}} G_{\mu\nu} G^{\mu\nu} O_U \quad (1)$$

Here  $f$  stands for a SM fermion and  $G^{\mu\nu}$  denotes the gauge field strength. Feynman rules for these operators have been given in [12]. The vertex functions generated from operators (1) are given by

$$i\frac{\lambda_S}{\Lambda_U^{d_U-1}}, \quad -\frac{\lambda_{PS}}{\Lambda_U^{d_U-1}}\gamma^5, \quad \frac{\lambda_V}{\Lambda_U^{d_U}}\gamma^\mu p_\mu, \quad 4i\frac{\kappa}{\Lambda_U^{d_U}}(-p_1 \cdot p_2 g^{\mu\nu} + p_1^\nu p_2^\mu), \quad (2)$$

where  $p$  is the unparticle momentum and  $p_1$  and  $p_2$  are the momenta of two photons. For convention, we assume that all the momenta are incoming to the vertex. The vertex  $\frac{\lambda_V}{\Lambda_U^{d_U}}\gamma^\mu p_\mu$  does not contribute to the process when the unparticle couples to a on-mass-shell fermion current. In some papers, it is assumed for simplicity that the coupling constants are all equal. To carry out a more general treatment we assume that they are different and distinguished by additional labels.

## II. SPIN DEPENDENT CROSS SECTION FOR $t\bar{t}$ PRODUCTION

The research and development on linear  $e^+e^-$  colliders have been progressing and the physics potential of these future machines is under study. After linear colliders are constructed its operating modes of  $e\gamma$  and  $\gamma\gamma$  are expected to be designed [13]. A real gamma beam is obtained through Compton backscattering of laser light off linear electron beam where most of the photons are produced at the high energy region. The luminosities for  $e\gamma$  and  $\gamma\gamma$  collisions turn out to be of the same order as the one for  $e^+e^-$  [14], so the cross sections for photoproduction processes with real photons are considerably larger than virtual photon case.

The spectrum of the backscattered photons is given by [14]

$$f_{\gamma/e}(y) = \frac{1}{g(\zeta)} \left[ 1 - y + \frac{1}{1-y} - \frac{4y}{\zeta(1-y)} + \frac{4y^2}{\zeta^2(1-y)^2} \right], \quad (3)$$

where

$$g(\zeta) = \left( 1 - \frac{4}{\zeta} - \frac{8}{\zeta^2} \right) \ln(\zeta + 1) + \frac{1}{2} + \frac{8}{\zeta} - \frac{1}{2(\zeta + 1)^2}, \quad (4)$$

with  $\zeta = 4E_e E_0 / M_e^2$ .  $E_0$  is the energy of the initial laser photon and  $E_e$  is the energy of the initial electron beam before Compton backscattering.  $y$  is the fraction which represents

the ratio between the scattered photon and the initial electron energy for the backscattered photons moving along the initial electron direction. The maximum value of  $y$  reaches 0.83 when  $\zeta = 4.8$  in which the backscattered photon energy is maximized without spoiling the luminosity.

The integrated cross section for  $t\bar{t}$  production via  $\gamma\gamma$  fusion can be obtained by the following integration:

$$d\sigma(e^+e^- \rightarrow \gamma\gamma \rightarrow t\bar{t}) = \int_{z_{min}}^{z_{max}} dz 2z d\hat{\sigma}(\gamma\gamma \rightarrow t\bar{t}) \int_{z^2/y_{max}}^{y_{max}} \frac{dy}{y} f_{\gamma/e}(y) f_{\gamma/e}(z^2/y) \quad (5)$$

where  $d\hat{\sigma}(\gamma\gamma \rightarrow t\bar{t})$  is the cross section of the subprocess and the center of mass energy of the  $e^+e^-$  system  $\sqrt{s}$ , is related to the center of mass energy of the  $\gamma\gamma$  system  $\sqrt{\hat{s}}$ , by  $\hat{s} = z^2 s$ .

In the presence of the couplings (2),  $\gamma\gamma \rightarrow t\bar{t}$  scattering is described by three tree-level diagrams. One can see from Fig.1 that the s-channel diagram contains unparticle exchange and modifies the SM amplitudes.

Since the top quark is very heavy, its helicity is frame dependent and changes under a boost from one frame to another. The helicity and chirality states do not coincide with each other and there is no reason to believe that the helicity basis will give the best description of the spin of the top quarks. Therefore, it is reasonable to study other spin bases better than helicity for the top quark spin. The spin four-vector of a top quark is defined by

$$s_t^\mu = \left( \frac{\vec{p}_t \cdot \vec{s}'}{m_t}, \vec{s}' + \frac{\vec{p}_t \cdot \vec{s}'}{m_t(E_t + m_t)} \vec{p}_t \right) \quad (6)$$

where  $(s_t^\mu)_{RF} = (0, \vec{s}')$  in the top quark rest frame. The laboratory frame is the  $e^+e^-$  center of mass system where the cross section is performed.  $\vec{s}'$  should be obtained by a Lorentz boost from the laboratory frame:

$$\vec{s}' = \lambda \frac{\vec{p}^\star}{|\vec{p}^\star|}, \quad \lambda = \pm 1. \\ \vec{p}^\star = \vec{p} + \frac{\gamma - 1}{\beta^2} (\vec{\beta} \cdot \vec{p}) \vec{\beta} - E \gamma \vec{\beta} \quad (7)$$

Here  $\vec{p}$  is the momentum of the particle moving along the top spin direction in the laboratory frame and  $\vec{p}^\star$  is the momentum observed in the rest frame of the top quark. A similar treatment can also be done for antitop quarks.

We consider two different top spin directions in the laboratory frame; one of the incoming photon beam direction and the helicity basis. We have calculated the polarized cross sections for the above spin directions of the top and unpolarized antitop quark. Calculations for polarized antitop and unpolarized top quark would lead to similar results. Phase space integrations have been taken by a Monte Carlo routine. In the cross section calculations we have performed a boost to obtain  $\vec{p}^*$  at each point in phase space.

Spin dependent SM squared amplitudes are given by

$$|M_1|^2 = \frac{4g_e^4}{27(q_1^2 - m_t^2)^2} \left\{ 8k_1 \cdot p_t k_1 \cdot p_{\bar{t}} + 16m_t^2 k_1 \cdot p_t + 8m_t^2 k_1 \cdot p_{\bar{t}} - 16m_t^4 - 8m_t^2 k_1 \cdot p_t s_t \cdot s_{\bar{t}} \right. \\ \left. + 8m_t^4 s_t \cdot s_{\bar{t}} - 8m_t^2 s_t \cdot k_1 s_{\bar{t}} \cdot k_1 + 8m_t^2 s_t \cdot k_1 s_{\bar{t}} \cdot p_t - 8m_t^2 p_t \cdot p_{\bar{t}} \right\} \quad (8)$$

$$|M_2|^2 = |M_1|^2 \quad (k_1 \longleftrightarrow k_2) \quad (9)$$

$$2 \operatorname{Re}(M_1^\dagger M_2) = \frac{32g_e^4}{27(q_1^2 - m_t^2)(q_2^2 - m_t^2)} \left\{ -m_t^2 k_1 \cdot p_{\bar{t}} + 2m_t^2 k_2 \cdot p_t - m_t^2 k_2 \cdot p_{\bar{t}} - m_t^4 \right. \\ - k_1 \cdot p_{\bar{t}} k_2 \cdot p_t s_t \cdot s_{\bar{t}} - m_t^2 k_2 \cdot p_t s_t \cdot s_{\bar{t}} + m_t^4 s_t \cdot s_{\bar{t}} + k_2 \cdot p_t s_t \cdot p_{\bar{t}} s_{\bar{t}} \cdot k_1 \\ + k_2 \cdot p_{\bar{t}} s_t \cdot k_1 s_{\bar{t}} \cdot p_t - m_t^2 s_t \cdot k_1 s_{\bar{t}} \cdot p_t + k_1 \cdot p_{\bar{t}} s_t \cdot k_2 s_{\bar{t}} \cdot p_t - m_t^2 s_t \cdot k_2 s_{\bar{t}} \cdot p_t \\ + m_t^2 s_t \cdot p_{\bar{t}} s_{\bar{t}} \cdot p_t + 2k_2 \cdot p_t p_t \cdot p_{\bar{t}} + m_t^2 p_t \cdot p_{\bar{t}} - m_t^2 s_t \cdot s_{\bar{t}} p_t \cdot p_{\bar{t}} - s_t \cdot k_2 s_{\bar{t}} \cdot k_1 \\ \times p_t \cdot p_{\bar{t}} - s_t \cdot k_1 s_{\bar{t}} \cdot k_2 p_t \cdot p_{\bar{t}} + k_1 \cdot p_t (2m_t^2 - k_2 \cdot p_{\bar{t}} s_t \cdot s_{\bar{t}} - m_t^2 s_t \cdot s_{\bar{t}} + s_t \cdot p_{\bar{t}} s_{\bar{t}} \cdot k_2 \\ \left. + 2p_t \cdot p_{\bar{t}}) + k_1 \cdot k_2 (m_t^2 (-1 + 2s_t \cdot s_{\bar{t}}) - s_t \cdot p_{\bar{t}} s_{\bar{t}} \cdot p_t + (-2 + s_t \cdot s_{\bar{t}}) p_t \cdot p_{\bar{t}}) \right\} \quad (10)$$

where  $k_1$  and  $k_2$  are the momenta of incoming photons,  $p_t$  and  $p_{\bar{t}}$  are the momenta of outgoing top and antitop quarks and  $s_t^\mu$  and  $s_{\bar{t}}^\mu$  are the spin four-vectors of top and antitop quarks. The u-channel amplitude can be obtained from the t-channel by interchanging the incoming photon momenta ( $k_1 \longleftrightarrow k_2$ ).

The spin dependent unparticle contributions are given by the following amplitudes:

$$|M_3|^2 = \frac{3A_{dU}^2}{\sin^2(\pi d_U)} |q_3^2|^{2d_U-4} \left( \frac{\kappa^2}{\Lambda_{dU}^{4d_U-2}} \right) \left\{ \lambda_S^2 \left[ 2(k_1 \cdot k_2)^2 (-m_t^2 + s_t \cdot p_{\bar{t}} s_{\bar{t}} \cdot p_t \right. \right. \\ \left. + p_t \cdot p_{\bar{t}} + s_t \cdot s_{\bar{t}} (m_t^2 - p_t \cdot p_{\bar{t}})) \right] + \lambda_{PS}^2 \left[ 2(k_1 \cdot k_2)^2 (m_t^2 - s_t \cdot p_{\bar{t}} s_{\bar{t}} \cdot p_t \right. \\ \left. + p_t \cdot p_{\bar{t}} + s_t \cdot s_{\bar{t}} (m_t^2 + p_t \cdot p_{\bar{t}})) \right] \right\}, \quad (11)$$

$$\begin{aligned}
2 \operatorname{Re}(M_1^\dagger M_3) = & -\frac{8 g_e^2 A_{d_U} |q_3^2|^{d_U-2}}{3 \sin(\pi d_U)} \frac{1}{(q_1^2 - m_t^2)} \left( \frac{\kappa}{\Lambda_U^{2d_U-1}} \right) \\
& \times \{ \lambda_S [m_t (k_2 \cdot p_t (k_1 \cdot p_t - k_1 \cdot p_{\bar{t}} - (k_1 \cdot p_t - k_1 \cdot p_{\bar{t}}) s_t \cdot s_{\bar{t}} \\
& - s_t \cdot p_{\bar{t}} s_{\bar{t}} \cdot k_1 + s_t \cdot k_1 s_{\bar{t}} \cdot p_t) + k_1 \cdot k_2 (s_t \cdot p_{\bar{t}} s_{\bar{t}} \cdot k_1 - s_t \cdot k_1 s_{\bar{t}} \cdot p_t \\
& + s_t \cdot p_{\bar{t}} s_{\bar{t}} \cdot p_t + s_t \cdot s_{\bar{t}} (k_1 \cdot p_t - k_1 \cdot p_{\bar{t}} + m_t^2 - p_t \cdot p_{\bar{t}}) - k_1 \cdot p_t + k_1 \cdot p_{\bar{t}} \\
& - m_t^2 + p_t \cdot p_{\bar{t}})) \cos(\pi d_U) - ((k_1 \cdot k_2 - k_2 \cdot p_t)(-1 + s_t \cdot s_{\bar{t}}) \epsilon^{k_1 p_t p_{\bar{t}} s_{\bar{t}}} \\
& + k_1 \cdot k_2 (s_{\bar{t}} \cdot p_t \epsilon^{k_1 p_{\bar{t}} s_t s_{\bar{t}}} - s_{\bar{t}} \cdot k_1 \epsilon^{p_t p_{\bar{t}} s_t s_{\bar{t}}}) + k_2 \cdot p_t (-s_{\bar{t}} \cdot p_t \epsilon^{k_1 p_{\bar{t}} s_t s_{\bar{t}}} \\
& + s_{\bar{t}} \cdot k_1 \epsilon^{p_t p_{\bar{t}} s_t s_{\bar{t}}})) \sin(\pi d_U)] + \lambda_{PS} [m_t \cos(\pi d_U) (k_2 \cdot p_t (\epsilon^{k_1 p_t s_t s_{\bar{t}}} \\
& + \epsilon^{k_1 p_{\bar{t}} s_t s_{\bar{t}}}) - k_1 \cdot k_2 (\epsilon^{k_1 p_t s_t s_{\bar{t}}} + \epsilon^{k_1 p_{\bar{t}} s_t s_{\bar{t}}} + \epsilon^{p_t p_{\bar{t}} s_t s_{\bar{t}}})) - (k_1 \cdot k_2 \\
& \times (-m_t^2 s_t \cdot k_1 + k_1 \cdot p_t s_t \cdot p_{\bar{t}} + m_t^2 s_t \cdot p_{\bar{t}} + m_t^2 s_{\bar{t}} \cdot k_1 - k_1 \cdot p_{\bar{t}} s_{\bar{t}} \cdot p_t \\
& + m_t^2 s_{\bar{t}} \cdot p_t - s_t \cdot k_1 p_t \cdot p_{\bar{t}} + s_{\bar{t}} \cdot k_1 p_t \cdot p_{\bar{t}}) + k_2 \cdot p_t (-k_1 \cdot p_t s_t \cdot p_{\bar{t}} \\
& - m_t^2 s_{\bar{t}} \cdot k_1 + k_1 \cdot p_{\bar{t}} s_{\bar{t}} \cdot p_t - s_{\bar{t}} \cdot k_1 p_t \cdot p_{\bar{t}} + s_t \cdot k_1 (m_t^2 + p_t \cdot p_{\bar{t}}))) \\
& \times \sin(\pi d_U)] \} , \tag{12}
\end{aligned}$$

$$2 \operatorname{Re}(M_2^\dagger M_3) = 2 \operatorname{Re}(M_1^\dagger M_3) (k_1 \longleftrightarrow k_2), \tag{13}$$

where  $A_{d_U} \equiv \frac{16\pi^{\frac{5}{2}}}{(2\pi)^{2d_U}} \frac{\Gamma(d_U + \frac{1}{2})}{\Gamma(d_U - 1)\Gamma(2d_U)}$ . The trigonometric functions  $\cos(\pi d_U)$  and  $\sin(\pi d_U)$  in the amplitudes (12) and (13) originate from the complex phase associated with the s-channel propagator and may lead to interesting interference effects with the standard model amplitudes.

The integrated cross section as a function of the unparticle couplings  $\kappa$ ,  $\lambda_S$  and  $\lambda_{PS}$  for various top quark spin polarizations are plotted in Figs. 2 - 6. In the figures the center of mass energy of the  $e^+e^-$  system is  $\sqrt{s}=1$  TeV.  $\sigma$  versus  $\kappa$  graphs are plotted under the assumption that  $\lambda_S=\lambda_{PS}=1$ . In the graphs of  $\sigma$  versus  $\lambda_S$  and  $\sigma$  versus  $\lambda_{PS}$ ,  $\kappa$  is taken to be 1;  $\lambda_{PS}$  and  $\lambda_S$  are taken to be zero, respectively. We see from these figures that the deviation of the cross section from its SM value increases with decreasing  $d_U$ . This is very clear from the factors  $\frac{1}{\Lambda_U^{4d_U-2}}$  and  $\frac{1}{\Lambda_U^{2d_U-1}}$  in the squared amplitudes (11)-(13). The influence of spin polarization on the behavior of the cross sections can be observed from the figures.

### III. ANGULAR CORRELATIONS BETWEEN TOP DECAY PRODUCTS AND SENSITIVITY LIMITS ON THE UNPARTICLE COUPLINGS

Top quark spin polarization can be determined from the angular distributions of its decay products. We consider the dominant decay chain of the top quark to leptons in the standard model,  $t \rightarrow W^+ b (W^+ \rightarrow l^+ \nu)$ . The differential cross section for the complete process including subsequent top decay is given by

$$d\sigma(\gamma\gamma \rightarrow t\bar{t} \rightarrow b\ell^+\nu_\ell\bar{t}) = \frac{1}{2s}|M|^2 \frac{d^3p_1}{(2\pi)^3 2E_1} \frac{d^3p_2}{(2\pi)^3 2E_2} \frac{d^3p_3}{(2\pi)^3 2E_3} \frac{d^3p_{\bar{t}}}{(2\pi)^3 2E_{\bar{t}}} \times (2\pi)^4 \delta^4(k_1 + k_2 - p_1 - p_2 - p_3 - p_{\bar{t}}), \quad (14)$$

where  $k_1$  and  $k_2$  are the momenta of the incoming photons,  $p_1$ ,  $p_2$  and  $p_3$  are the momenta of the outgoing fermions and  $p_{\bar{t}}$  is the momentum of the outgoing antitop quark.  $|M|^2$  is the square of the full amplitude which is averaged over the initial spins and summed over the final spins. The full amplitude can be expressed as follows:

$$|M|^2 (2\pi)^4 \delta^4(k_1 + k_2 - p_1 - p_2 - p_3 - p_{\bar{t}}) = \int \frac{d^4q}{(2\pi)^4} \left| \sum_{s_t} M_a(s_t) D_t(q^2) M_b(s_t) \right|^2 \times (2\pi)^4 \delta^4(k_1 + k_2 - p_{\bar{t}} - q) \times (2\pi)^4 \delta^4(q - p_1 - p_2 - p_3), \quad (15)$$

where  $q$  and  $s_t$  are the internal momentum and spin of the top quark.  $D_t(q^2)$  is the Breit-Wigner propagator factor.  $M_a(s_t)$  is the amplitude for the process  $\gamma\gamma \rightarrow t\bar{t}$  with on shell  $t$  quark.  $M_b(s_t)$  is the decay amplitude for  $t \rightarrow b\ell^+\nu_\ell$ . The square of the decay amplitude summed over the final fermion spins is given by

$$|M_b(s_t)|^2 = \frac{2g_w^4}{[(p_t - p_b)^2 - m_w^2]^2} (p_b \cdot p_t - p_b \cdot p_\ell)(p_\ell \cdot p_t - m_t(s_t \cdot p_\ell)) \quad (16)$$

Here  $p_\ell$  and  $p_b$  are the momenta of the final lepton and  $b$  quark.

It is easy to show that interference terms from different spin states will vanish after integrating the decay part in (15) over azimuthal angles of the top quark decay products. Then the full cross section can be written as a product of production and decay parts. Using

the narrow width approximation and after some simple algebra, the following result can be obtained:

$$d\sigma(\gamma\gamma \rightarrow t\bar{t} \rightarrow b\ell^+\nu_\ell\bar{t}) = \left[ d\sigma(\gamma\gamma \rightarrow \uparrow t\bar{t}) \frac{d\Gamma(\uparrow t \rightarrow b\ell^+\nu_\ell)}{\Gamma(t \rightarrow b\ell^+\nu_\ell)} + d\sigma(\gamma\gamma \rightarrow \downarrow t\bar{t}) \frac{d\Gamma(\downarrow t \rightarrow b\ell^+\nu_\ell)}{\Gamma(t \rightarrow b\ell^+\nu_\ell)} \right] BR(t \rightarrow b\ell^+\nu_\ell), \quad (17)$$

where  $BR(t \rightarrow b\ell^+\nu_\ell)$  is the leptonic branching ratio for the top quark. Up and down arrows indicate spin up and spin down cases along a specified spin quantization axis respectively.  $d\Gamma(\uparrow t \rightarrow b\ell^+\nu_\ell)$  and  $d\Gamma(\downarrow t \rightarrow b\ell^+\nu_\ell)$  are the differential decay rates for the polarized top quarks. The unpolarized rate is given by;  $d\Gamma(t \rightarrow b\ell^+\nu_\ell) = d\Gamma(\uparrow t \rightarrow b\ell^+\nu_\ell) + d\Gamma(\downarrow t \rightarrow b\ell^+\nu_\ell)$ . For a fixed top quark spin, polarized production cross sections can be obtained from a fit to the polar angle distribution of the top decay product, an outgoing charged lepton in the top rest frame. To be precise, the polarized production cross sections  $d\sigma(\gamma\gamma \rightarrow \uparrow t\bar{t})$  or  $d\sigma(\gamma\gamma \rightarrow \downarrow t\bar{t})$  can be obtained from a fit to the  $d\Gamma(\uparrow t \rightarrow b\ell^+\nu_\ell)$  or  $d\Gamma(\downarrow t \rightarrow b\ell^+\nu_\ell)$  distributions (17).

It is important to reconstruct the rest frame of the top quark, since this is essential for its polarization identification. Since it is impossible to detect a neutrino from a decaying top quark, it is difficult to reconstruct the top quark momentum. On the other hand the top momentum can be reconstructed from the antitop momentum and the momenta of the incoming photons. We assume that the antitop quark is unpolarized; therefore, semi-leptonic decay is not a necessary assumption for the antitop quark. Hence it is reliable to assume that the antitop momentum is reconstructable. Reconstruction of incoming photon momenta can be achieved by means of very forward detectors in the ILC. Detection of the Compton backscattered electron and positron, scattered at an almost zero-degree angle, in the very forward detectors allow us to reconstruct the Compton backscattered photon momenta. This kind of measurement was performed by the H1 collaboration at HERA, but for Weizsacker-Williams photons from the electron or proton [15]. In the LHC, it is foreseen that one may equip two LHC experiments, ATLAS and CMS, with very forward detectors which allow one to detect intact scattered protons at very small angles after the collision. Therefore, it is reasonable to assume a similar very forward detector equipment for the ILC [16].



As a concrete result; we have obtained 95% confidence level limits on the unparticle couplings  $\kappa$ ,  $\lambda_S$  and  $\lambda_{PS}$  using a simple  $\chi^2$  analysis at  $\sqrt{s}=1$  TeV and an integrated luminosity  $L_{int} = 500 fb^{-1}$  without systematic errors. The  $\chi^2$  function is given by

$$\chi^2 = \left( \frac{\sigma_{SM} - \sigma(\kappa, \lambda_S, \lambda_{PS})}{\sigma_{SM} \delta} \right)^2, \quad (18)$$

where  $\delta = \frac{1}{\sqrt{N}}$  is the statistical error. The expected number of events has been calculated considering the leptonic decay channel of the W boson as the signal  $N = AL_{int}B(t \rightarrow W^+b(W^+ \rightarrow l^+\nu))B(\bar{t} \rightarrow W^-\bar{b}(W^- \rightarrow l^-\bar{\nu}))\sigma$ , where  $A$  is the overall acceptance.

The limits on the unparticle couplings are given in Tables I-III with an acceptance of  $A = 0.7$ . This acceptance value is assumed for the b-tagging efficiency as in references [17]. On the other hand, using an acceptance of 0.5 instead of 0.7 does not spoil our limits more than by a factor of 1.17. In Table I we consider unpolarized top quark and in Tables II and III we consider various top quark spin polarizations. We omit the limits on the scalar coupling  $\lambda_S$  for the polarized top quark, since  $\lambda_S$  is insensitive to the polarization. Limits on  $\kappa$  have been calculated under the assumption that  $\lambda_S=\lambda_{PS}=1$ , and limits on  $\lambda_S$  and  $\lambda_{PS}$  have been calculated under the assumption that  $\kappa=1$  and the other remaining coupling is zero. We see from the tables that significant improvements are obtained in the sensitivity bounds by taking into account top quark spin polarization for large values of the scale dimension  $d_U \in [1, 2]$ . For instance, the helicity right spin polarization configuration of the top improves the lower bound on  $\kappa$  by the factors of 7.5, 12.8 and 12 for  $d_U=1.5$ ,  $d_U=1.7$  and  $d_U=1.9$ , respectively. Helicity right improves the lower bound, and helicity left improves the upper bound on  $\lambda_{PS}$  by a same factor of 4 for  $d_U=1.7$ . These improvement factors are 2.3, 3.8 and 3.2 for  $d_U=1.3$ ,  $d_U=1.5$  and  $d_U=1.9$ . It is observed from the tables that the improvement factors decrease as  $d_U$  decreases and approaches to 1. This behavior is reasonable from the analytic expressions of the interference terms (12) and (13). The interference of unparticle contributions with the SM amplitudes explicitly depends on the scale dimension  $d_U$  via its trigonometric functions. Therefore any variation in  $d_U$  should produce some interference effects like the one which we have observed from the tables. We see from expressions (12) and (13) that interference terms are odd functions of the unparticle couplings. Therefore, these interference effects spoil the symmetric behavior of the cross section in the negative and positive intervals of the unparticle couplings. Of course, it is very difficult to predict the

effect of an interference contribution from the analytic expressions (12) and (13) precisely. But numerical results show that the improvement provided by the polarization generally increases as  $d_U$  increases for  $\kappa$  and  $\lambda_{PS}$ . We observe from Figs.2-6 that deviation of the cross section from the SM for  $d_U=1.5$  depends significantly on the polarization for  $\kappa$  and  $\lambda_{PS}$ . Altering the spin orientations, spin up to down or helicity right to left, significantly changes the behavior of the cross sections as a function of the couplings  $\kappa$  or  $\lambda_{PS}$  for  $d_U=1.5$ . This is very compatible with the results in the tables.

Another useful quantity about spin-induced angular correlations, one that may be sensitive to new physics is the spin asymmetry,

$$A_{\uparrow\downarrow} = \frac{N_{\uparrow} - N_{\downarrow}}{N_{\uparrow} + N_{\downarrow}} \quad (19)$$

Here the subscript up arrow  $\uparrow$  (down arrow  $\downarrow$ ) stands for spin up (spin down), and  $N$  represents the number of events for the corresponding spin. Substituting the spin dependent amplitude square (16), into (17) and after some algebra we can reach the following expression:

$$\frac{1}{\sigma_T} \frac{d\sigma}{d\cos\theta} = \frac{1}{2}(1 + A_{\uparrow\downarrow}\cos\theta), \quad (20)$$

where  $\theta$  is defined as the angle between the charged lepton (from the decaying top quark) and the top quark spin quantization axis in the rest frame of the top quark.

Spin asymmetry is a significant observable about spin-induced angular correlations. The polarization of the top quark can be extracted from the  $\cos\theta$  distribution in (20). We see from (20) that the up or down polarization state of the top quark is determined by the sign of  $\cos\theta$ . The size of the spin asymmetry shows how we can easily observe angular correlations and therefore the polarized cross sections.

In table IV we have presented spin asymmetries for the helicity basis and one of the incoming photon beam direction. In the table, the unparticle couplings are taken to be  $\kappa=1$ ,  $\lambda_S=0$  and  $\lambda_{PS}=1$ . Spin asymmetries for  $\kappa=1$ ,  $\lambda_S=1$  and  $\lambda_{PS}=0$  are all zero, so we have not presented them in the table. The zero spin asymmetry for  $\kappa=1$ ,  $\lambda_S=1$  and  $\lambda_{PS}=0$  exhibits that the scalar coupling  $\lambda_S$  is insensitive to the polarization. On the other hand, this information provides us the opportunity to dissociate  $\lambda_{PS}$  from  $\lambda_S$  by studying the top spin asymmetries.

## IV. CONCLUSIONS

We have investigated the potential of  $\gamma\gamma \rightarrow t\bar{t}$  with polarized top quarks to probe the scalar unparticle top and scalar unparticle photon couplings. The most sensitive results are obtained for  $d_U=1.1$ . The sensitivity limits get worse as the  $d_U$  increases. This is clear from the inverse powers of the energy scale  $\Lambda_U$  and common in most processes. On the other hand, top spin polarization leads to a significant improvement to the sensitivity limits for large values of  $d_U \in [1, 2]$ .

We have also investigated the effect of the unparticle couplings on the spin asymmetries. We show that the spin asymmetries are insensitive to the scalar coupling  $\lambda_S$ . On the other hand, they are sensitive to the pseudoscalar coupling  $\lambda_{PS}$ , and the spin asymmetries are large for large values of  $d_U$ . Therefore, at least in principle, it is possible to dissociate  $\lambda_{PS}$  from  $\lambda_S$  by measuring the top spin asymmetry in  $\gamma\gamma \rightarrow t\bar{t}$ .

## Acknowledgments

The author acknowledges support through the Scientific and Technical Research Council (TUBITAK) BIDEB-2219 grant.

- 
- [1] T. Banks and A. Zaks, Nucl. Phys. **B196**, 189 (1982).
  - [2] H. Georgi, Phys. Rev. Lett. **98**, 221601 (2007).
  - [3] H. Georgi, Phys. Lett. **B650**, 275 (2007).
  - [4] K. Cheung, W.-Y. Keung and T.-C. Yuan, Phys. Rev. Lett. **99**, 051803 (2007); M. Luo and G. Zhu, arXiv:0704.3532 [hep-ph]; C.H. Chen and C. Q. Geng, arXiv:0705.0689 [hep-ph]; Y. Liao, arXiv:0705.0837 [hep-ph]; G.J. Ding and M.L. Yan, arXiv:0705.0794 [hep-ph]; T.M. Aliev, A.S. Cornell and N. Gaur, arXiv:0705.1326 [hep-ph]; X.Q.Li and Z.T. Wei, Phys. Lett. **B651**, 380 (2007); M.A. Stephanov, Phys. Rev. **D76**, 035008 (2007); N. Greiner, arXiv:0705.3518 [hep-ph]; S.L. Chen and X.G. He, Phys. Rev. **D76**, 091702 (2007); T.M. Aliev, A.S. Cornell and N. Gaur, JHEP **0707**, (2007); P. Mathews and V. Ravindran, arXiv:0705.4599 [hep-ph]; S. Zhou, arXiv:0706.0302 [hep-ph]; G.J. Ding and M.L. Yan, arXiv:0706.0325 [hep-ph]; C.H. Chen and C.Q. Geng, arXiv:0706.0850 [hep-ph]; M. Bander, J.L. Feng, A. Rajaraman and Y. Shirman,

- arXiv:0706.2677 [hep-ph]; T.G. Rizzo, arXiv:0706.3025 [hep-ph]; S.L. Chen, X.G. He and H.C. Tsai, JHEP **11**, 010 (2007); R. Zwicky, arXiv:0707.0677 [hep-ph]; T. Kikuchi and N. Okada, arXiv:0707.0893 [hep-ph]; R. Mohanta and A.K. Giri, arXiv:0707.1234 [hep-ph]; C.S. Huang and X.H. Wu, arXiv:0707.1268 [hep-ph]; N.V. Krasnikov, arXiv:0707.1419 [hep-ph]; A. Lenz, arXiv:0707.1535 [hep-ph]; D. Choudhury and D.K. Ghosh, arXiv:0707.2074 [hep-ph]; A. Delgado, J. R. Espinosa and M. Quiros, arXiv:0707.4309 [hep-ph]; M. Neubert, arXiv:0708.0036 [hep-ph]; G. Bhattacharyya, D. Choudhury and D.K. Ghosh, arXiv:0708.2835 [hep-ph]; Y. Liao, arXiv:0708.3327 [hep-ph]; S. Majhi, arXiv:0709.1960 [hep-ph]; A. Kobakhidze, Phys. Rev. D **76**, 097701 (2007); A. B. Balantekin and K. O. Ozansoy, arXiv:0710.0028 [hep-ph]; O. Cakir, K. O. Ozansoy, arXiv:0710.5773 [hep-ph]; I. Sahin and B. Sahin, arXiv:0711.1665 [hep-ph]; K. Cheung, C. S. Li and T.-C. Yuan, arXiv:0711.3361 [hep-ph]; R. Mohanta and A.K. Giri, arXiv:0711.3516 [hep-ph]; K. Huitu and S. K. Rai, arXiv:0711.4754 [hep-ph]; O. Cakir, K. O. Ozansoy, arXiv:0712.3814 [hep-ph]; Y. Wu and D.-X. Zhang, arXiv:0712.3923 [hep-ph]; T. Kikuchi, N. Okada and M. Takeuchi, arXiv:0801.0018 [hep-ph]; X.-G. He and S. Pakvasa, arXiv:0801.0189 [hep-ph]; C.-H. Chen, C. S. Kim and Y. W. Yoon, arXiv:0801.0895 [hep-ph]; J. L. Feng, A. Rajaraman and H. Tu, arXiv:0801.1534 [hep-ph]; C.-F. Chang, K. Cheung, T.-C. Yuan, arXiv:0801.2843 [hep-ph]; M. J. Aslam and Cai-Dian Lu, arXiv:0802.0739 [hep-ph].
- [5] H. Davoudiasl, arXiv:0705.3636 [hep-ph]; A. Freitas and D. Wyler, JHEP **12**, **033** (2007); S. Hannestad, G. Raffelt and Yvonne Y. Y. Wong, arXiv:0708.1404v1 [hep-ph]; P. K. Das, arXiv:0708.2812v2 [hep-ph]; L. Anchordoqui and H. Goldberg, arXiv:0709.0678 [hep-ph]; J. McDonald, arXiv:0709.2350 [hep-ph]; I. Lewis, arXiv:0710.4147 [hep-ph]; G. L. Alberghi, A.Yu. Kamenshchik, A. Tronconi, G.P. Vacca and G. Venturi, arXiv:0710.4275 [hep-th]; S.-L. Chen, X.-G. He, X.-P. Hu and Y. Liao, arXiv:0710.5129 [hep-ph]; T. Kikuchi and N. Okada, arXiv:0711.1506 [hep-ph]; S. Dutta and A. Goyal, arXiv:0712.0145 [hep-ph].
- [6] R. D. Peccei, X. Zhang, Nucl. Phys. **B337**, 269 (1990);  
R. D. Peccei, S. Peris and X. Zhang, Nucl. Phys. **B349**, 305 (1991).
- [7] A. T. Alan and N. K. Pak, arXiv:0708.3802 [hep-ph]; A. T. Alan, N. K. Pak and A. Senol, arXiv:0710.4239 [hep-ph].
- [8] H.-F. Li, H.-L. Li, Z.-G. Si and Z.-J. Yang, arXiv:0802.0236 [hep-ph].
- [9] I. Bigi, Y. Dokshitzer, V. Khoze, J. Kuhn and P. Zerwas, Phys. Lett. **B 181**, 157 (1986).
- [10] K. Y. Lee, S. C. Park, H. S. Song, J. Song and C. Yu, Phys. Rev. D **61**, 074005 (2000); M.

- Arai, N. Okada, K. Smolek and V. Simak, Phys. Rev. D**70**, 115015 (2004); M. Arai, N. Okada, K. Smolek and V. Simak, Phys. Rev. D**75**, 095008 (2007).
- [11] G. A. Ladinsky and C.-P. Yuan, Phys. Rev. D**49**, 9 (1994); P. Poulose and S. D. Rindani, Phys. Rev. D**54**, 7 (1996); M. S. Baek, S. Y. Choi and C. S. Kim, Phys. Rev. D**56**, 11 (1997); P. Poulose and S. D. Rindani, Phys. Rev. D**57**, 9 (1998); B. Grzadkowski and Z. Hioki, Phys. Rev. D**61**, 014013 (1999); Z.H. Lin, T. Han, T. Huang, J.-X. Wang and X. Zhang, Phys. Rev. D**65**, 014008 (2001).
- [12] K. Cheung, W.-Y. Keung and T.-C. Yuan, Phys. Rev. D**76**, 055003 (2007).
- [13] C. Akerlof, Ann Arbor Report No. UM HE 81-59 (1981);  
J. A. Aguilar-Saavedra *et al.*, TESLA Technical Design Report, DESY-2001-011.
- [14] I.F. Ginzburg *et al.*, Nucl. Instrum. Methods **205**, 47 (1983); *ibid.* **219**, 5 (1984).
- [15] F. D. Aaron *et al.* (H1 Collaboration), arXiv:0810.3096 [hep-ex]; S. Chekanov *et al.* (ZEUS Collaboration), Eur. Phys. J. C **55**, 177191 (2008).
- [16] J. de Favereau *et al.*, CP3-08-04; K. Piotrkowski, Phys. Rev. D **63** 071502(R) (2001); V. P. Gonçalves and M. V. T. Machado, Phys. Rev. C **73** 044902 (2006); Phys. Rev. D **75**, 031502(R) (2007).
- [17] Puneet Batra and Tim M. P. Tait, Phys. Rev. D **74**, 054021 (2006); S. S. Biswal *et al.*, Phys. Rev. D**73**, 035001 (2006) ; D. Choudhury and Mamta, Phys. Rev. D**74**, 115019 (2006).

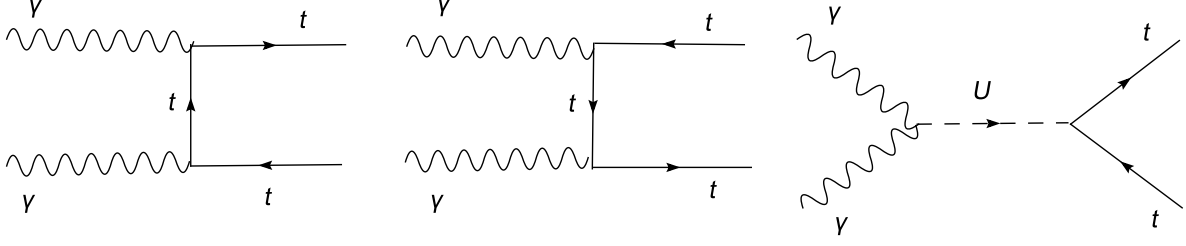


FIG. 1: Tree-level Feynman diagrams for  $\gamma\gamma \rightarrow t\bar{t}$  in the presence of scalar unparticle couplings.

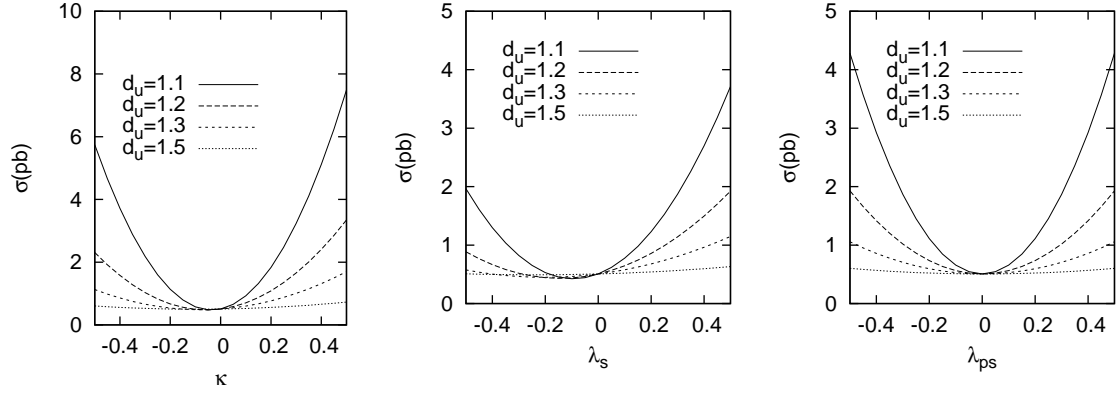


FIG. 2: The integrated cross section of  $\gamma\gamma \rightarrow t\bar{t}$  as a function of the unparticle couplings  $\kappa$ ,  $\lambda_S$  and  $\lambda_{PS}$  for an unpolarized top-antitop quark pair. Legends are for various values of the scale dimension  $d_U$  and  $\sqrt{s} = \Lambda_U = 1$  TeV.

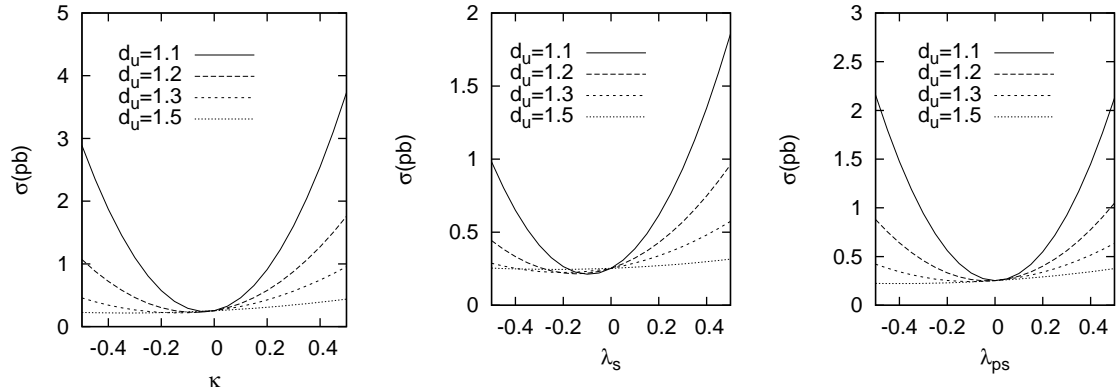


FIG. 3: The same as Fig.2, but the top quark is in the helicity basis with left helicity and the antitop quark is unpolarized.

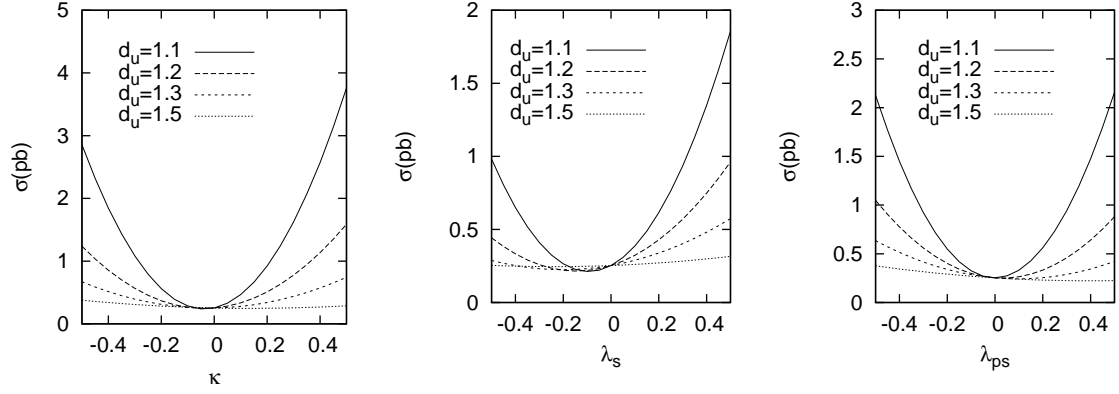


FIG. 4: The same as Fig.3, but the top quark is in the right helicity state.

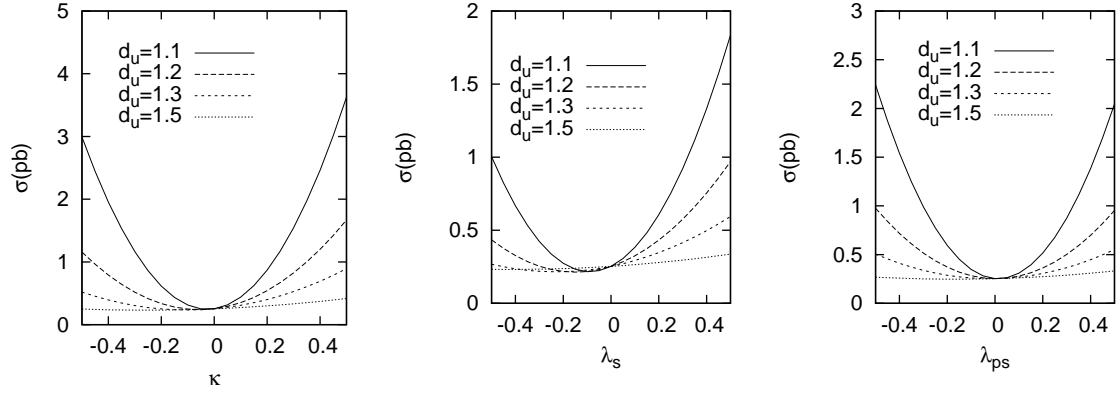


FIG. 5: The same as Fig.4, but the top quark spin decomposition axis is along one of the incoming photon beam direction. The spin orientation of the top quark is spin up and the antitop quark is unpolarized.

TABLE I: Sensitivity of  $\gamma\gamma \rightarrow t\bar{t}$  to unparticle couplings at 95% C.L. for various scale dimensions. Top and antitop quarks are unpolarized. The center of mass energy of the  $e^+e^-$  system is  $\sqrt{s} = 1$  TeV and  $L_{int} = 500 fb^{-1}$ . The unparticle energy scale is taken to be  $\Lambda_U = 1$  TeV.

	$d_U = 1.1$	$d_U = 1.3$	$d_U = 1.5$	$d_U = 1.7$	$d_U = 1.9$
$\kappa$	-0.049, 0.008	-0.171, 0.015	-0.458, 0.033	-0.880, 0.067	-0.794, 0.086
$\lambda_S$	-0.117, 0.009	-0.413, 0.016	-1.050, 0.034	-2.062, 0.070	-1.798, 0.092
$\lambda_{PS}$	-0.025, 0.025	-0.065, 0.065	-0.158, 0.158	-0.316, 0.316	-0.341, 0.341

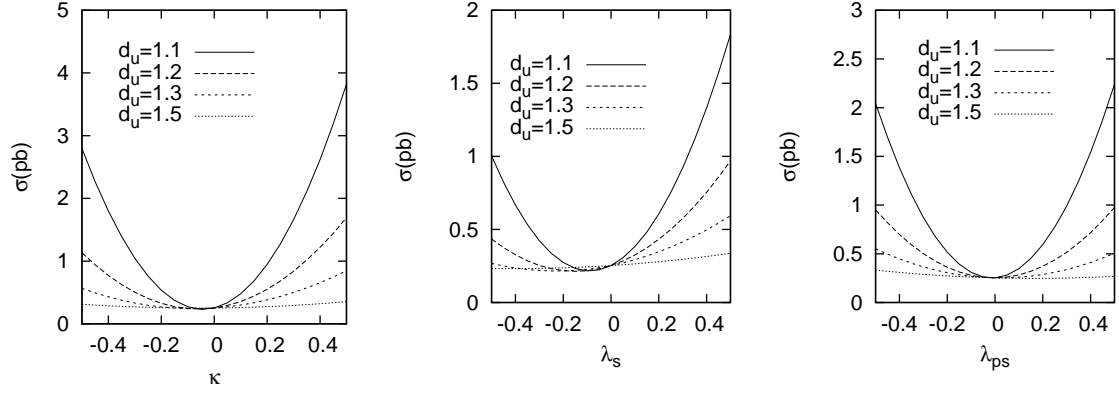


FIG. 6: The same as Fig.5 but spin orientation of the top quark is spin down.

TABLE II: Sensitivity of  $\gamma\gamma \rightarrow t\bar{t}$  to unparticle coupling  $\kappa$  at 95% C.L. for various spin decomposition axes of the top and unpolarized antitop quark. The center of mass energy of the  $e^+e^-$  system is  $\sqrt{s} = 1$  TeV and  $L_{int} = 500 fb^{-1}$ . The unparticle energy scale is taken to be  $\Lambda_U = 1$  TeV.

Spin Top	$\kappa$ ( $d_U = 1.1$ )	$\kappa$ ( $d_U = 1.3$ )	$\kappa$ ( $d_U = 1.5$ )	$\kappa$ ( $d_U = 1.7$ )	$\kappa$ ( $d_U = 1.9$ )
$\gamma$ -beam					
Up	-0.061, 0.009	-0.222, 0.016	-0.566, 0.037	-0.634, 0.132	-0.282, 0.343
Down	-0.090, 0.006	-0.176, 0.021	-0.222, 0.095	-0.795, 0.105	-1.127, 0.086
Helicity					
Right	-0.080, 0.007	-0.084, 0.044	-0.061, 0.344	-0.069, 1.187	-0.066, 1.453
Left	-0.076, 0.007	-0.288, 0.013	-0.702, 0.030	-1.012, 0.083	-0.483, 0.260

TABLE III: The same as Table II, but for unparticle coupling  $\lambda_{PS}$ .

Spin Top	$\lambda_{PS}$ ( $d_U = 1.1$ )	$\lambda_{PS}$ ( $d_U = 1.3$ )	$\lambda_{PS}$ ( $d_U = 1.5$ )	$\lambda_{PS}$ ( $d_U = 1.7$ )	$\lambda_{PS}$ ( $d_U = 1.9$ )
$\gamma$ -beam					
Up	-0.019, 0.045	-0.101, 0.059	-0.419, 0.084	-1.132, 0.124	-1.002, 0.165
Down	-0.045, 0.019	-0.059, 0.101	-0.084, 0.419	-0.124, 1.132	-0.165, 1.002
Helicity					
Right	-0.032, 0.028	-0.028, 0.220	-0.042, 0.839	-0.078, 1.808	-0.107, 1.533
Left	-0.028, 0.032	-0.220, 0.028	-0.839, 0.042	-1.808, 0.078	-1.533, 0.107



TABLE IV: Spin asymmetries for helicity basis and one of the incoming photon beam direction. The unparticle couplings are taken to be  $\kappa=1$ ,  $\lambda_S=0$  and  $\lambda_{PS}=1$ . The center of mass energy of the  $e^+e^-$  system is  $\sqrt{s}=1$  TeV and  $\Lambda_U=1$  TeV.

Scale Dimension	$A_{\uparrow\downarrow}$ (Helicity Basis)	$A_{\uparrow\downarrow}$ ( $\gamma$ Beam Direction)
$d_U=1.1$	0.004	-0.025
$d_U=1.3$	-0.157	0.034
$d_U=1.5$	-0.342	0.144
$d_U=1.7$	-0.274	0.160
$d_U=1.9$	-0.197	0.116